Title: Grainstone cross-set geometry as a physical proxy for chemical and biological sediment cohesion

Authors: Benjamin T. Cardenas*, Benjamin P. Smith

Jackson School of Geosciences, University of Texas at Austin, Austin, TX, USA

Now at Division of Geological and Planetary Sciences, California Institute of Technology, Pasadena, CA, USA

Resubmitted to Geology, original manuscript #G46929

*Corresponding Author Information

Telephone: (210) 240-0382

Email: bencard@caltech.edu

Pages: 13

Characters (title through fig. captions, 18,500 limit) 18,243

Abstract: words (250 word limit) 234

Figures: 4 (4 figure limit)

References: 35

Grainstone cross-set geometry as a physical proxy for chemical and biological sediment cohesion

Benjamin T. Cardenas*, Benjamin P. Smith

Jackson School of Geosciences, University of Texas at Austin, Austin, TX, USA

Now at Division of Geological and Planetary Sciences, California Institute of Technology, Pasadena, CA, USA

ABSTRACT

Preserved cross-set thicknesses are powerful tools for unravelling past environmental conditions. The relative rate of bedform aggradation to migration (climb angle) is encoded into the distribution of cross-set thicknesses. In siliciclastic settings, climb angles have been used to reconstruct properties of the depositional system, including ancient topography, which exerts a control on local aggradation rates. Cross-set thickness distributions in carbonate environments should prove equally useful. Carbonate sediments are often bound by early cements or microbes, both of which influence sediment transport. If cross sets record these interactions, then they may contain information about local—and possibly global—changes to sediment cohesion.

To test this idea, we analyzed the distribution of cross-set thicknesses in a grainstone interval of the Cretaceous Glen Rose Formation at an outcrop in Austin, TX, USA. Bedform climb angles inferred from the distribution of cross-set thicknesses were on the order of 0.5° to 5°. In siliciclastic systems, climb angles this high are typically driven by the filling of local relief; relief is minor in this carbonate system. We interpret this as evidence for rapid bed aggradation driven by early cements or organic binding, a boundary condition of potential significance to carbonate depositional settings. We suggest that at geologic time scales, global trends in carbonate bedform preservation should be sensitive to both carbonate chemistry and biotic innovations. If so, our results provide a quantitative method for exploring these topics in deep time.

INTRODUCTION

The migration and aggradation of dunes become encoded into the thicknesses of the associated sets of cross strata (Paola and Borgman, 1991; Jerolmack and Mohrig, 2005). Dune migration and aggradation are sensitive to external boundary conditions including changing sediment availability and antecedent topography, as well as internal autogenic factors (e.g., Ganti et al., 2013; Reesink et al., 2015; Mahon and McElroy, 2018; Swanson et al., 2017, 2019). To a point, the coupling of cross-set thicknesses to dune kinematics appears to be agnostic of general depositional setting (Jerolmack and Mohrig, 2005a; Cardenas et al., 2019). However, the relevant boundary conditions driving bedform kinematics are highly dependent on depositional setting, making cross-strata analysis widely informative.

While cross-set aggradation usually results from spatial decelerations in the flow, recent work suggests that grain-to-grain binding by organic or physiochemical processes may produce a similar result by effectively increasing the threshold of sediment motion (Parsons et al., 2016). For example, low concentrations (<1%) of organic polymers can create "bridges" between grains, reducing sediment mobility and bedform size compared to organic-free sediments (Malarkey et al., 2015). Furthermore, shallow-water carbonate settings experience additional binding in the form of syndepositional cements and crusts (Moore et al., 1973; Lamb et al., 2012). These cements may be inorganic or instead associated with the aforementioned polymers (e.g., Visscher et al., 2000). Thus, it is possible that bedform kinematics in carbonate systems—and, by extension, their cross-set thicknesses—record biological and chemical boundary conditions that are perhaps negligible or non-existent in siliciclastic settings. Here, we test this hypothesis using cross-stratified grainstones from the Cretaceous Glen Rose Formation, Austin, TX, USA, and comparing their set thicknesses to those in siliciclastic strata.

METHODS

The roadcut exposing the Glen Rose Formation grainstones studied here is located along the eastern side of Highway 360 in Austin, Texas, USA, located at 30.3332° N, 97.8072° W (Fig. 1A). A scaled photopan of the outcrop was built by flattening 38 high-resolution photos to a plane, imaging an area 30 m long by 1.2 m high with mm-scale resolution, and allowed for the mapping of bounding surfaces, as well as the identification of grainstone versus mudstone on the basis of sedimentary structures, roughness, and protrusion, informed by field examination. Thickness measurements of grainstone beds were made along 69 vertical sections with 0.36 m spacing (best practice is as close as possible, Paola and Borgman, 1991). The distribution of set thicknesses ($\underline{s}$) was then compared to fitted exponential and gamma curves using a two-sample Kolmogorov-Smirnov test. The coefficient of variation ($\underline{c}_v$) for set thicknesses was calculated as

$$\underline{c}_v = \underline{s}_\sigma / \underline{s}_m \quad (1),$$

where $\underline{s}_m$ and $\underline{s}_\sigma$ are the mean and standard deviation of the measured set thicknesses. This method quantifies the significance of bed aggradation in the construction of the deposit. Assuming bedform heights were gamma distributed as is often observed in siliciclastic bedforms (Paola and Borgman, 1991; van der Mark et al., 2008; Ganti et al., 2013), a system undergoing net bypass (zero net bed aggradation) will have a $\underline{c}_v = 0.88$ and exponentially distributed set thicknesses (Paola and Borgman, 1991). The creation of any record at all in this scenario is dependent on the variability in scour depths, and is limited to the fills of the deepest scours (Paola and Borgman, 1991). Bed aggradation, forced by a spatial deceleration driven by some external or internal process, creates a gamma distribution of set thicknesses and a lower $\underline{c}_v$, as preservation is not limited to the thickest and thinnest sets. With significant aggradation, the set thickness gamma distribution and $\underline{c}_v$ reflect those of the formative bedform heights (Jerolmack and Mohrig, 2005). Cross-set lengths and bounding surface relief were measured as well.

RESULTS

The outcrop shows a consistent vertical arrangement of facies ~5.4 m thick, shown in the vertical log in Figure 1. Facies D (Fig. 1C) is the focus of the 1.2 m high panorama and is exposed continuously across it (Fig. 2A and S1). Mapped surfaces bound the cross-bedded grainstone interval, as well as individual cross sets and mudstone drapes within the interval (Fig. 1C). The mean length of a cross set is 3.33 m, ~62 times mean set thickness, while bounding surfaces have a mean relief of 83 mm and a standard deviation of 71 mm. Dolomitized mudstones lacking mudcracks within the cross-bedded grainstone interval fill local lows (Fig. 2A), as well as draping topographic highs (Fig. 2B). The drapes and plugs compose 9% of this facies. Rippled grainstone surfaces are preserved within these mudstones (Fig. 3A). The cross beds contain rip-up clasts of the dolomitized mudstone throughout (Fig. 3B). The top of the laminated mudstone below the grainstone interval follows the relief of the laminations with few deep truncations of the laminated interval (Fig. 3C).

The distribution of cross-set thicknesses ($n = 727$) have $\underline{s_m} = 68$ mm, $\underline{s_\sigma} = 34$ mm, and $\underline{c_v} = 0.50$ (Eq. 1), and is shown as a cumulative distribution function (CDF; Fig. 4A) and a probability density function (PDF; Fig. 4B) along with fitted distributions. The gamma distribution is not rejected at a significance level of 0.05 ($p = 0.70$), while the exponential fit is rejected ($p < 0.001$).

DISCUSSION

Depositional setting and bedform kinematics

The facies succession records two cycles (Fig. 1C). The first shallowing-upward cycle coarsens upwards from mud-dominated packstones (MDP) (A) to grain-dominated packstones (GDP) (B) before passing into laminated mudstones which are interpreted as microbial laminations in a peritidal environment (C; Pratt, 2010). The next hemicycle deepens upwards, passing from cross-bedded grainstones with mudstone drapes and plugs (D) to burrowed grainstone (E), and wackestone (F). The final hemicycle shallows again from wackestone (F) to GDP (G) (Tucker, 1985). Together, these cycles suggest meter-scale water depth changes in a subtidal to supratidal environment. Given the compound nature of the grainstone interval composed of smaller cross-sets, and the interbedded mudstone drapes and plugs without mudcracks (Figs. 3A-B), the cross-bedded grainstone interval (D) is interpreted to represent a subtidal bar (Gonzalez and Eberli, 1997). The 9% mudstone content measured in this interval is similar to the mud content observed in modern tidal bars (Reeder and Rankey, 2008). A tidal bar interpretation also fits with previous interpretations of a shallow, restricted inner platform at this location during deposition of the upper Glen Rose Formation (Phelps et al., 2014).

A relatively high ratio of aggradation rate to bedform migration rate (i.e., climb angle) was required to construct these cross sets as indicated by the good fit of the gamma distribution, the rejection of the exponential fit, the lateral continuity of sets relative to their thickness, and the low c_v of 0.50, associated with climb angles on the order of 0.5° to 5° (Fig. 4A-B; Jerolmack and Mohrig, 2005). Rapid bed aggradation is also supported by the spatial relationships between mudstone and grainstone. Mudstone drapes are preserved over topographically low and high parts of the bar (Figs. 3A-B), yet mudstone rip-ups ubiquitous throughout the grainstone interval (Figs. 2B and 3B) suggest transport conditions were capable of re-mobilizing these drapes. Drapes over high relief would be particularly susceptible to reworking. An interpretation consistent with these observations and the quantitative analysis is that aggradation was rapid enough to remove these drapes from the active scouring zone before complete reworking could occur. Finally, the continuity of the cross sets (Fig. 2B) is inconsistent with a low aggradation rate model, which should produce significant lateral variability in set thickness and the complete truncation of cross sets by other cross sets (Jerolmack and Mohrig, 2005; Cardenas et al., 2019). Although these all indicate significant aggradation rates, there is no evidence of sediment-starved bedforms.

In siliciclastic settings where similar c_v values and aggradational architectures are recorded, aggradation was driven by the spatial deceleration of bedforms into local topographic lows (Reesink et al., 2015; Cardenas et al. 2019). Local topography is certainly capable of exerting a control on carbonate deposition (Puga-Bernabéu et al., 2014; Kocurek et al., 2019), but the studied interval shows no indicators of a topographic control, such as a thickening of sets climbing into depressions larger than the sets, or downlapping. Instead, mean bounding-surface relief is similar to mean set thickness. Additionally, the presence of intertidal facies such as microbial laminites indicates that accommodation was extremely limited. Another possible scenario is aggradation was forced by a deceleration related to tides. Continuous, rapidly accumulated sets in the siliciclastic record are sometimes associated with bars in river-dominated deltas (Enge et al., 2010; Fidolini and Ghissani, 2016). Siliciclastic tidal-bar strata are not as continuous, and reworking is observed on at least the time scale of spring tides (twice monthly; Fenies and Tastet, 1998). Indeed, a lack of reworking in other strata has been attributed to early carbonate cementation (Nelson et al., 1988; Puga-Bernabéu et al., 2014). In either case, the high c_v value for the carbonate grainstone, in the absence of a clear topographic driver for spatial deceleration and preservation, likely reflects a non-negligible boundary condition of this carbonate environment.

The presence of both rip-up clasts (Fig. 3B) and adjacent microbial laminites (Fig. 3C) point to this boundary condition: the grain-to-grain binding of sediments by organic polymers or mineral growth. Microbial biomass decreases erosion rates even when cohesive surface mats are not present (Chen et al., 2017; Malarkey et al., 2015). This process appears to be especially relevant in tidal environments; both numerical modeling (Mariotti and Fagherazzi, 2012) and experimental work (Mariotti et al., 2014) suggest that microbes can colonize bedforms on the scale of days to weeks, allowing them to gain a foothold during neap tidal cycles. The other process, cementation by carbonate growth, is common in many shallow-water carbonate environments (Shinn et al., 1969; Moore et al., 1973; Vousdoukas et al., 2007). Rapid cementation of this facies is generally supported by the preserved ripples within the mudstone plug, which we interpret to have been lithified enough by the time of their burial to prevent deformation (Figs. 3A and 4C). We interpret the high climb angles as the result of one or both binding processes that decrease sediment mobility. Based on the $\underline{c}_v$ of 0.50, sediment trapping at the bed drove bed aggradation at rates of 0.01 to 0.1 times the average bedform migration rate (Jerolmack and Mohrig, 2005, their Fig. 4B), producing the high climb angles observed here (Fig. 4C).

Implications for the evolution of marine substrates

Measurements of set thicknesses, especially in carbonates, provides a metric for detecting subtle changes in sediment fluxes and bedform kinematics due to ambient biological or chemical processes. While biological effects are well-documented in flume experiments, most studies focus on plan-form bedform shape as a record of kinematics (e.g., Malarkey et al., 2015; Parsons et al., 2016). In contrast, vertical views of cross-bedded deposits are much more common in the geologic record. Techniques for analyzing cross-set thickness should provide a wealth of information about the relationships among bedform kinematics, biology, carbonate chemistry, and paleo-ocean temperatures (Nelson and James, 2000).

As noted by Parsons et al., (2016), bedform kinematics might even enhance our global view of life and Earth’s biogeochemical cycles. For example, many ancient carbonates suggests that cohesive substrates—as evidenced by stromatolites, crystal fans, and flat-pebble conglomerates—are tied to major changes in ocean chemistry and life (e.g., Grotzinger and James, 2000). Set thicknesses can complement and extend these analyses to substrates that are not fully cohesive, providing a common framework that can be applied across shallow-water settings of all ages. The current study provides a proof-of-concept that variations in set thickness between deposits with evidence for binding (i.e., nearby microbialites and rip ups) are measurably different from settings where binding is negligible.

CONCLUSIONS

Physical sedimentologic processes are important for fully understanding carbonate rocks (Lamb et al., 2012; Trower et al., 2017). Syndepositional seafloor cementation and biological grain binding can exert a significant control on the accumulation and preservation of cross-bedded grainstone strata, where these forcings become encoded into the distribution of cross-set thicknesses. Thus, set thickness distributions may be a unique and complimentary physical proxy for understanding the chemical and biological evolution of marine substrates. The collection of these data may be especially critical for the majority of history where direct geochemical proxies are ambiguous or poorly preserved.

ACKNOWLEDGEMENTS

We acknowledge C. Kerans, D. Mohrig, R. Grmela, and the students of UT-Austin’s 2018 Carbonate and Evaporite Depositional Settings course for their help with this work.

FIGURE CAPTIONS

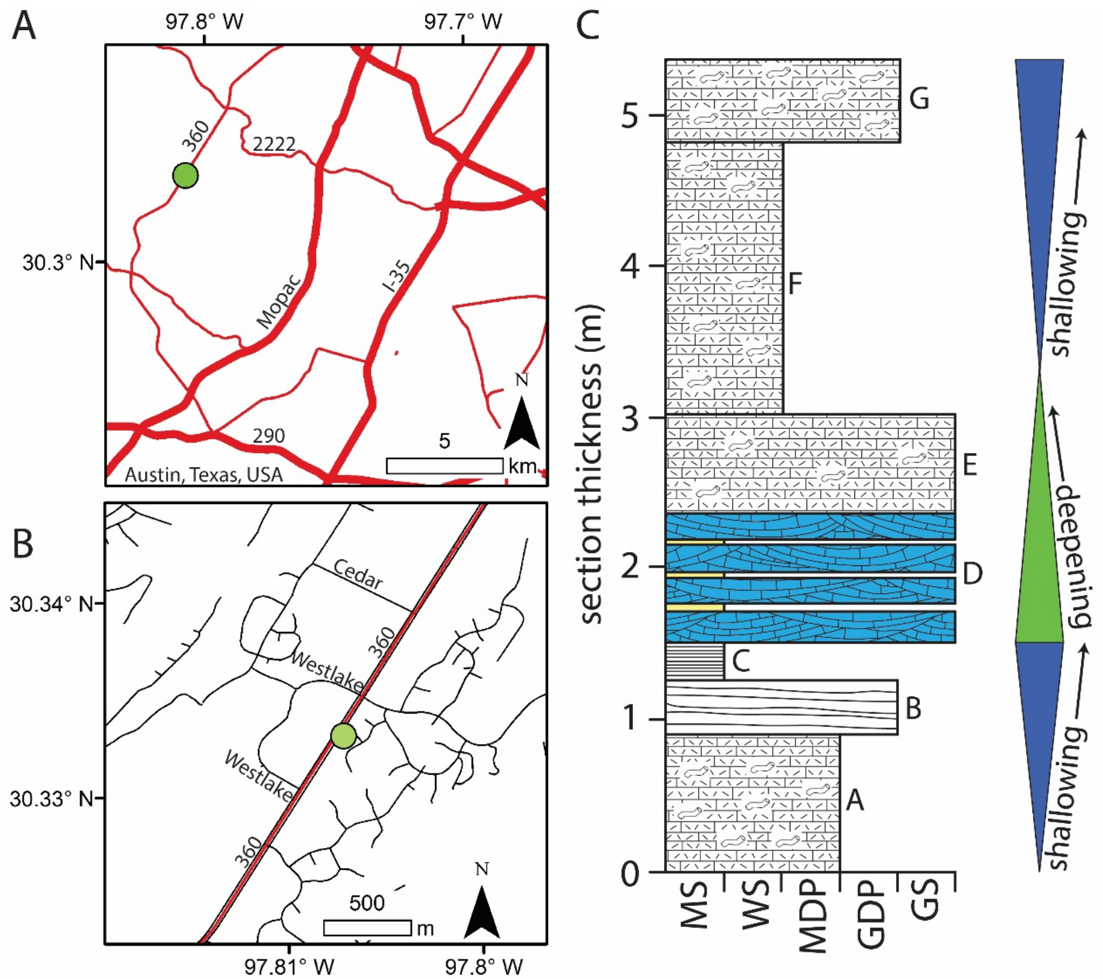

Figure 1 - A: Locality map of Austin, TX, with outcrop location at the green dot. Labels and red lines show major highways. B: Zoom in to local roads around the outcrop (green dot). Street and highway maps from Texas Department of Transportation. C: The outcrop shows a consistent vertical arrangement of facies ~5.4 m thick, labeled A-G from bottom to top: A: Burrowed mud-dominated packstone (MDP; ~0.9 m). B: Laminated grain-dominated packstone (GDP; ~0.4 m). C: Microbial laminated mudstone (MS; 0.3 m). D: cross-bedded GS MS plugs and drapes (~0.8 m); E: Partially burrowed GS (~0.7 m); F: Burrowed wackestone (WS; ~1.8 m); G: Burrowed GDP (0.5 m). Facies D, colored in blue, is the focus of the 1.2 m high panorama and is exposed continuously across it (Fig. 2A). Interpreted shallowing and deepening hemicycles are shown to the side.

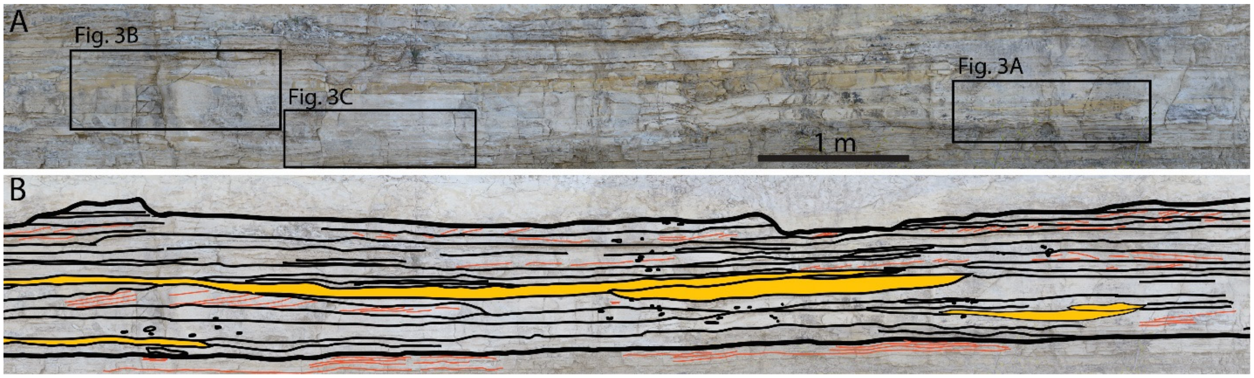

Figure 2 - A: Representative subset of the cross-bedded grainstone and mudstone interval. Locations of panels 3A-C are shown. B: Interpretation of panel A with bounding surfaces mapped in thin black lines and larger mudstone drapes colored in yellow. Smaller mudstone drapes were omitted from this interpretation, but were not included in thickness analysis. The top and bottom of the interval are mapped with bold black lines. Cross strata within the interval are mapped in orange. Orange lines beneath the interval follow the microbial laminations below. Small black circles outline mudstone rip-up clasts seen more clearly in the full-sized panorama (Fig. S1).

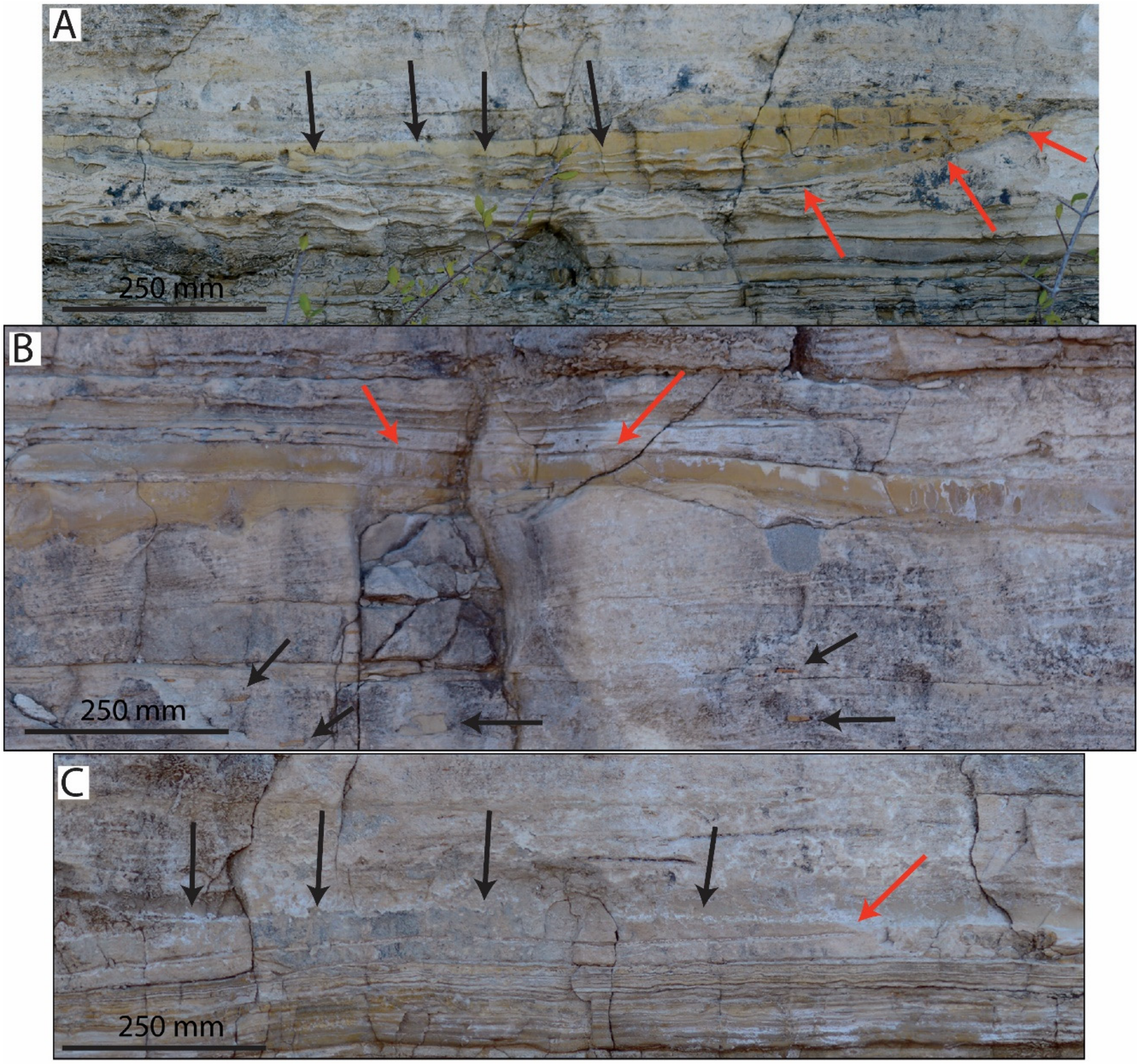

Figure 3 - Key observations recording the unusually complete preservation and rapid aggradation of this interval. A: Mudstones preserved in topographic lows (red arrows) contain within them undeformed rippled grainstone surfaces (black arrows). B: Mudstone rip-up clasts within grainstone beds (black arrows) indicate flows were capable of reworking local deposits, yet mudstones still drape topographic highs (red arrows). C: Grainstone contact with microbial laminites below follows the laminations (black arrows) with some local scour (red arrow).

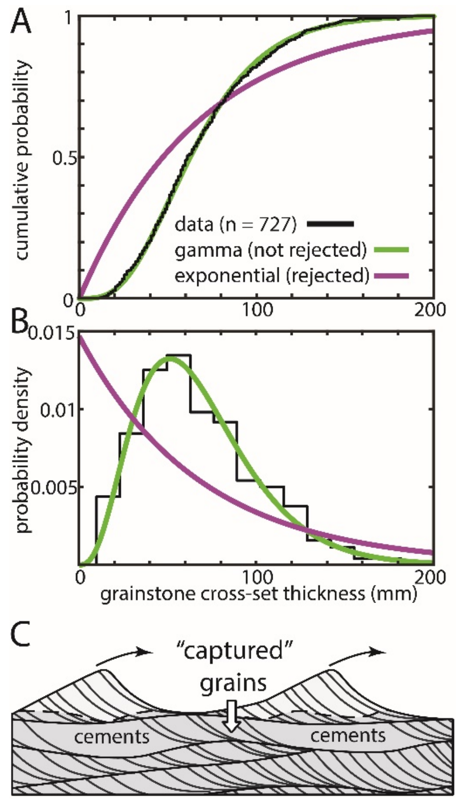

Figure 4 – A and B: Cumulative distribution (A) and probability density (B) function comparisons of gamma and exponential fits to set thickness data. The gamma fit is not rejected, indicating bedform climb was significant (Jerolmack and Mohrig, 2005, their Fig. 4B). The exponential fit is rejected. (C) Bedforms migrating through a region undergoing syndepositional cementation. Surface cements capture the grains at bedform troughs, inhibiting their reworking, driving troughs upward, and promoting high climb angles.

Fig. S1 – The complete panorama showing the cross-bedded grainstone interval. The locations of panels in Figures 2 and 3 are shown. A: Uninterpreted panorama. B: Interpreted panorama, with grainstone boundaries mapped in thick black lines, set boundaries mapped in thin black lines, cross strata and laminations mapped in thin red lines, and major mud drapes and plugs mapped in solid yellow.

REFERENCES CITED

Bridge, J., 1997, Thickness of sets of cross strata and planar strata as a function of formative bed-wave geometry and migration, and aggradation rate: Geology, v. 25, p. 971-974.

Bridge, J., and Best, J., 1997, Preservation of planar laminae due to migration of low-relief bed waves over aggrading upper-stage plane beds: comparison of experimental data with theory: Sedimentology, v. 44, p. 253-262.

Cardenas, B.T., Kocurek, G., Mohrig, D., Swanson, T., Hughes, C.M., and Brothers, S.C., 2019, Preservation of autogenic processes and allogenic forcings in set-scale aeolian architecture II: the scour-and-fill dominated Jurassic Page Sandstone, Arizona, USA: Journal of Sedimentary Research, v. 89, p. 741-760.

Chen, X.D., Zhang, C.K., Paterson, D.M., Thompson, C.E.L., Townend, I.H., Gong, Z., Zhou, Z., and Feng, Q., 2017, Hindered erosion: The biological mediation of noncohesive sediment behavior: Water Resources Research, v. 53, p. 4787–4801, doi:10.1002/2016WR020105.

Enge, H.D., Howell, J.A., and Buckley, S.J., 2010, Quantifying clinothem geometry in a forced-regressive river-dominated delta, Panther Tongue Member, Utah, USA: Sedimentology, v. 57, p. 1750-1770.

Fenies, H., and Tastet, J.-P., 1998, Facies and architecture of an estuarine tidal bar (the Trompeloup bar, Gironde Estuary, SW France): Marine Geology, v. 150, p. 149-169.

Fidolini, F., and Ghinassi, M., 2016, Friction- and intertia-dominated effluents in a lacustrine, river-dominated deltaic succession (Pliocene Upeer Valdarno Basin, Italy): Journal of Sedimentary Research, v. 86, p. 1083-1101.

Ganti, V., Paola, C., and Foufoula-Georgiou, E., 2013, Kinematic controls on the geometry of the preserved cross sets: Journal of Geophysical Research: Earth Surface, v. 118, p. 1296-1307.

Gonzalez, R., and Eberli, G.P., 1997, Sediment transport and bedforms in a carbonate tidal inlet; Lee Stocking Island, Exumas, Bahamas: Sedimentology, v. 44, p. 1015-1030.

Jerolmack, D.J., and Mohrig, D., 2005a, Frozen dynamics of migrating bedforms: Geology, v. 33, p. 57-60.

Jerolmack, D.J., and Mohrig, D., 2005b, A unified model for subaqueous bed form dynamics: Water Resources Research, v. 41, W12421.

Grotzinger, J.P., and James, N.P., 2000, Precambrian carbonates: Evolution of understanding, in Grotzinger, J.P., and James, N.P., eds., Carbonate sedimentation and diagenesis in the evolving Precambrian world: SEPM (Society for Sedimentary Geology) Special Publication 67, p. 3–20.

Kocurek, G., Martindale, R.C., Day, M., Goudge, T.A., Kerans, C., Hassenruck-Gudipati, H.J., Mason, J., Cardenas, B.T., Petersen E.I., Mohrig, D., Aylward, D.S., Hughes, C.M., and Nazworth, C.M., 2019, Antecedent aeolian dune topographic control on carbonate and evaporite facies: Middle Jurassic Todilto Member, Wanakah Formation, Ghost Ranch, New Mexico, USA: Sedimentology, v. 66, p. 808-837.

Lamb, M.P., Fischer, W.W., Raub, T.D., Perron, J.T., and Myrow, P.M., 2012, Origin of giant wave ripples in snowball Earth cap carbonate: Geology, v. 40, p. 827-830.

Malarkey, J., Baas, J.H., Hope, J.A., Aspden, R.J., Parsons, D.R., Peakall, J., Paterson, D.M., Schindler, L.Y., Lichtman, I.D., Bass, S.J., Davies, A.G., Manning, A.J., and Thorne, P.D., 2015, The pervasive role of biological cohesion in bedform development: Nature Communications, v. 6, p. 6257, doi:10.1038/ncomms7257.

Mariotti, G., and Fagherazzi, S., 2012, Modeling the effect of tides and waves on benthic biofilms: Journal of Geophysical Research: Biogeosciences, v. 117, doi:10.1029/2012JG002064.

Mariotti, G., Perron, J.T., and Bosak, T., 2014, Feedbacks between flow, sediment motion and microbial growth on sand bars initiate and shape elongated stromatolite mounds: Earth and Planetary Science Letters, v. 397, p. 93–100, doi:10.1016/j.epsl.2014.04.036.

Moore, C. H. Jr., 1973, Intertidal carbonate cementation, Grand Cayman, West Indies: Journal of Sedimentary Petrology, v. 43, p. 591-602.

Nelson, C.S., Keane, S.L., Head, D., 1988. Nontropical carbonate deposits on the modern New Zealand shelf. Sedimentary Geology 60, 71–94.

Nelson, C.S. and James, N.P., 2000. Marine cements in mid-Tertiary cool-water shelf limestones of New Zealand and southern Australia. Sedimentology 47, 609–629

Paola, C., and Borgman, L., 1991, Reconstructing random topography from preserved stratification: Sedimentology, v. 38, p. 553-565.

Parsons, D.R., Schindler, R.J., Hope, J.A., Malarkey, J., Baas, J.H., Peakall, J., Manning, A.J., Ye, L., Simmons, S., Patterson, D.M., Aspden, R.J., Bass, S.J., Davies, A.G., Lichtman, I.D., and Thorne, D.P., 2016, The role of biophysical cohesion on subaqueous bed form size: Geophysical Research Letters, v. 43, p. 1566–1573, doi:10.1002/2016GL067667.

Phelps, R.M., Kerans, C., Loucks, R.G., Da Gama, R.O., Jeremiah, J., and Hull, D., 2014, Oceanographic and eustatic control of carbonate platform evolution and sequence stratigraphy on the Cretaceous (Valanginian–Campanian) passive margin, northern Gulf of Mexico: Sedimentology, v. 61, p. 461–496.

Pratt, B.R., 2010, Peritidal Carbonates, Chapter 16 from Facies Models 4, ed. James, N.P., and Dalrymple, R.W., Geological Association of Canada.

Puga-Bernabéu, Á., Martín, J.M., Braga, J.C., Aguirre, J. 2014. Offshore remobilization processes and deposits in low-energy temperate-water carbonate-ramp systems: Examples from the Neogene basins of the Betic Cordillera (SE Spain). Sedimentary Geology 304, 11–27.

Reeder, S.L., and Rankey, E.C., 2008, Interactions between tidal flows and ooid shoals, Northern Bahamas: Journal of Sedimentary Research, v. 78, p. 175-186.

Reesink, A.J.H., van den Berg, J.H., Parsons, D.R., Amsler, M.L., Best, J.L., Hardy, R.J., Orfeo, O., and Szupiany, R.N., 2015, Extremes in dune preservation: Controls on the completeness of fluvial deposits: Earth-Science Reviews, v. 150, p. 652-665.

Shinn, E.A., 1969, Submarine lithification of Holocene carbonate sediments in the Persian Gulf: Sedimentology, v. 12, p. 109–144.

Swanson, T., Mohrig, D., Kocurek, G., and Liang, M., 2017, A surface model for aeolian dune topography: Mathematical Geosciences, v. 49, p. 635-655.

Swanson, T., Mohrig, D., Kocurek, G., Cardenas, B.T., and Wollinsky, M.A., 2019, Preservation of autogenic processes and allogenic forcings within set-scale aeolian architecture I: numerical experiments: Journal of Sedimentary Research, v. 89, p. 728-740.

Trower, E. J., Lamb, M. P., and Fischer, W. W., 2017, Experimental evidence that ooid size reflects a dynamic equilibrium between rapid precipitation and abrasion rates: Earth and Planetary Science Letters, v. 468, p. 112-118.

Tucker, M.E., 1985, Shallow-marine carbonate facies and facies models: Geological Society, London, Special Publications, v. 18, p. 147-169.

van der Mark, C.F., Blom, A., and Hulscher, S.J.M.H., 2008, Quantification of variability in bedform geometry: Journal of Geophysical Research, v. 113, F03020.

Visscher, P.T., Reid, R.P., and Bebout, B.M., 2000, Microscale observations of sulfate reduction: Correlation of microbial activity with lithified micritic laminae in modern marine stromatolites: , p. 4.

Vousdoukas, M.I., Velegrakis, A.F., and Plomaritis, T.A., 2007, Beachrock occurrence, characteristics, formation mechanisms and impacts: Earth-Science Reviews, v. 85, p. 23–46.